Buckling of Ge nanowires under uniaxial compression

Qingyuan Meng*, Yuhang Jing*

* Department of Astronautical Science and Mechanics, Harbin Institute of Technology, Harbin, 150001 PR China, jingyuhang@gmail.com

ABSTRACT

Molecular dynamics simulations are performed to investigate the buckling properties of [100]-, [110]-, [111]-, and [112]-oriented single-crystalline germanium nanowires under uniaxial compression. The effects of simulation temperature, strain rate, and wire length on the buckling behaviour are investigated. The simulation results indicate that critical load clearly decreases with increasing temperature and with decreasing strain rate. Additionally, the present results show that the critical load decreases with the increase of wire length, which is in agreement with the Euler theory.

Keywords: Ge nanowires; Molecular dynamics; Compression; Buckling

1 INTRODUCTION

Nanoscale one–dimensional structures, such as nanowires, nanotubes, and nanobelts, are of particular interest due to their unique properties and potential applications superior to their corresponding bulk form. Utilizing the structure at the nanometer level is a key technology in the development of electronic devices and elements of nano electromechanical systems (NEMS). Therefore, it is important to understand the mechanical properties for engineering usefulness such as design of reliability in service. Recently many materials have been used for the generation of nanotubes and nanowires [1-7]. Silicon nanowires appear to be an especially appealing choice due to their compatibility with conventional Si-based electronic technology [8-10]. Several correlative theoretical studies have been performed in recent years [11-16]. These studies involved the structural, electronic, optical, and mechanical properties of silicon nanowires along [100], [110], [111], and [112] orientations. It has been suggested that silicon nanowires can be a potential candidate for sensing and optical applications. It is well known that germanium (Ge) has many advantages over silicon for electronic applications [17]. Therefore, significant experimental and theoretical investigations of germanium nanowires (GeNWs) have been reported recently [18-25]. T.Hanrath and B.A.Korgel [18] have grown GeNWs along the [110], [111], and [112] directions with diameters as low as 3.7 nm. Jessica L.Lensch-Falk et al. [19] reported GeNWs along the [110], [111], and [112] directions with diameters of 17 to 32 nm. D.Medaboina et al. [25] have also investigated the structural, energetic, and electronic properties of hydrogen-passivated GeNWs along the [001], [110], and [111] directions, using first-principles calculations. Understanding the mechanical behavior of GeNWs is essential and of significant importance in order to determine the strength of the nanowires for practical application as electronic or optical devices. However to the best of our knowledge, a detailed study on the mechanical properties of GeNWs under uniaxial compression has not been performed before. In this work, the buckling behaviors of GeNWs with [100], [110], [111], and [112] crystallographic directions under compression are investigated by molecular dynamics simulations. The effects of temperature, strain rate, and wire length are systematically investigated.

2 SIMULATION DETAILS

Fig. 1 shows the representative cross-sections of the GeNWs with different growth directions. The geometry of the first plot in Fig. 1 is bounded by four (100) planes in all lateral directions and is oriented along [100] direction. The geometry of the second GeNWs (Fig. 1) is the same as those of the nanowires observed from experiments [18]. It is oriented along [110] direction and has a hexagonal cross-section with four (111) and two (100) lateral surfaces. The third one (Fig. 1) is oriented along [111] direction and all of its lateral directions are bounded by (110) planes. Finally, the geometry of the last one (Fig. 1) is similar to the GeNWs observed experimentally [18]. It is oriented along [112] direction and bounded by two (110) and two (111) surfaces in the lateral directions. To save computational time, the NWs are relatively thin with diameters of about 4 nm, which corresponds to the size of experimentally produced thinnest wire [18].

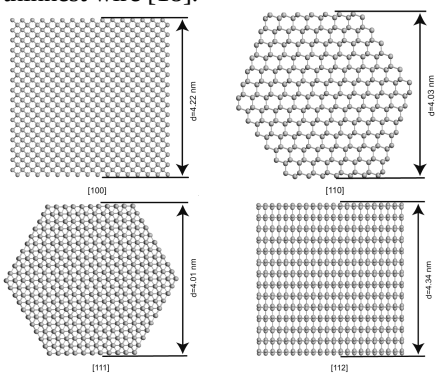

Fig.1. Cross-sections of the optimized structures of GeNWs in four different growth directions [100], [110], [111], and [112].

The atomic interactions are described using the Stillinger-Weber (SW) potential [26, 27]. The empirical SW interatomic potential consists of two- and three-body interaction terms and was originally fitted to describe the crystalline and liquid silicon phases. This potential consists of sums of two- and three-body interaction contributions. The two-body potential describes the formation of a chemical bond between two atoms. The three-body potential favors structures in which the angles between two bonds made by the same atom are close to the tetrahedral angle. The SW potential has been used in the study of germanium and found to give an excellent structural representation of amorphous solid Ge as well as crystalline Ge and give good results for several thermodynamic properties [27]. Recently, the SW potential has been adopted for the study of SiNWs and GeNWs, and found to give good results for nanowire properties [28-30]. Therefore, the SW potential should be reliable to study the mechanical properties of GeNWs.

The loading state in the present compression simulations is as follows: the loading is applied along the axis, and bottom and top layers are set as fixed layers; the others are set as thermal controlled layers. The system temperature is controlled by rescaling the atom velocities [31]. The GeNWs were initially annealed at 700 K over a period of 106 time-steps, where each step is separated by an interval of 0.5 fs, and then the structures of the nanowires were dynamically relaxed at a given temperature for 50 ps with traction-free boundary conditions, which allows the nanowires to have stable configuration. The strain was then applied along the wire direction to study the mechanical properties of the GeNWs. In order to investigate the relative influences of thermal effects, strain rates, and wire length on the mechanical properties of the current GeNWs under compression loading conditions, this study simulates testing under various temperatures in the range of 10 K to 900 K, with strain rates varying from 0.01%/ps to 0.5%/ps and wire length ranging from 16 nm to 32 nm.

3 RESULTS AND DISCUSSION

Figs. 2-5 show the axial load-strain relationship of the [100]-oriented NWs with length 32 nm, [110]-oriented NWs with length 32 nm, [111]-oriented NWs with length 32 nm, and [112]-oriented NWs with length 32 nm, respectively, simulated at 300 K, with strain rate of 0.02%/ps. Typical points where changes take place on the NWs' crystal structure and load-strain response were marked on the plot, indicated by numerical notations with angular brackets <>. From Figs. 2-5 we can see that the critical strains are 6.7%, 4.1%, 4.7%, and 5.9% for the [100]-, [110]-, [111]-, and [112]-oriented GeNWs. The four types of the nanowires buckle at different strains. The difference can be clarified by the bond configuration in crystalline germanium as shown in Fig. 6. As the strain is applied along the [100] direction (the bond configuration of crystalline germanium in the [001] direction is the same as that of crystalline germanium in the [001] direction), the bond angles $\angle Ge1OGe3$, $\angle Ge1OGe4$, $\angle Ge2OGe3$, and $\angle Ge2OGe4$ can decrease, whereas as the strain is applied along the [110] direction, only the $\angle Ge1OGe2$ decreases with the increasing strain, and the [111] and [112] directions are between the [001] and [110] directions, so the [100]-oriented NWs show largest critical strain. The young's modulus can be directly evaluated from the results of compressed tests with a lower strain (<2%). For the [100], [110], [111], and [112] directions, the Young's modulus of the NWs are 87.9, 96.8, 93.4, and 98.4 GPa, respectively. The values are consistent with the experimental result of 87-125 GPa of GeNWs [32, 33]. The results clearly show that nanowires of different directions have distinctly different Young's modulus. Therefore, it appears that both the electronic properties [25] and the mechanical properties of the GeNWs strongly depend on the orientation.

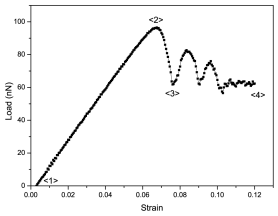

Fig.2.

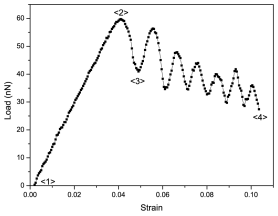

Fig.3.

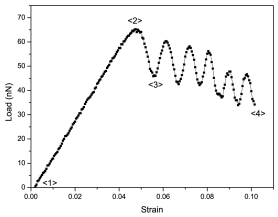

Fig.4.

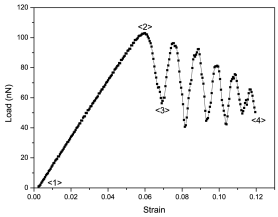

Fig.5.

Load-strain curves of [100], [110], [111], and [112]-oriented nanowires with length of 32 nm simulated at temperature 300 K and strain rate of 0.02%/ps.

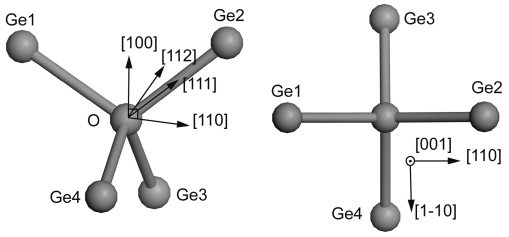

Fig.6. a Side view of bond configuration of crystalline germanium. b Top view of bond configuration of crystalline germanium.

Since buckling occurs as a result of dynamic processes, the mechanisms of material deformation are influenced both by temperature and by strain rate. Therefore, if material deformations in GeNWs are to be fully understood, the influences of these factors must be investigated. Fig. 7 shows the effects of temperature and strain rate on the

buckling behavior. Fig. 7(a) shows the variation in critical load with the temperature for the four types of GeNWs. The results clearly demonstrate that the critical buckling load decreases at higher temperature. At higher temperature, the atomic structure has high entropy, and the atoms vibrate about their equilibrium position at much larger amplitude, a greater number of molecules gain sufficient energy to overcome the activation energy barrier, as compared to low temperature, and hence deformation occurs. This result suggests that a thermally activated process plays an activating role in the buckling of GeNWs. Fig 7(b) shows the variation in critical load with the strain rate for the four types of GeNWs. It is seen that the buckling load and the strain rate are approximately linearly related. The present results clearly demonstrate that the mechanical properties of GeNWs are sensitive to the strain rate and temperature conditions.

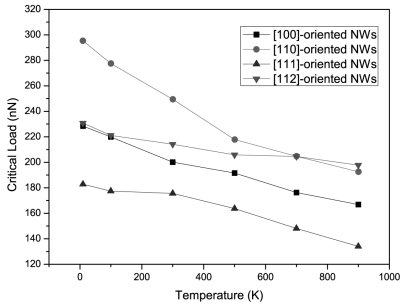

(a) The variation in critical load with the temperature for the four types of GeNWs.

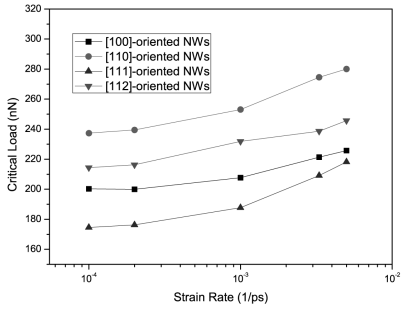

(b) The variation in critical load with the strain rate for the four types of GeNWs.

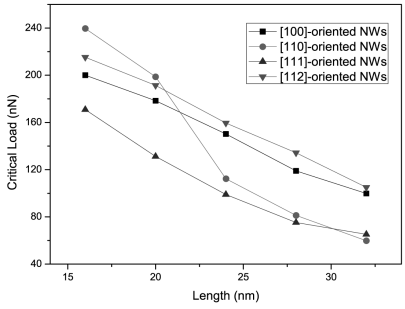

Fig.7 (c) The variation in critical load with the length for the four types of GeNWs.

In general, under compression two kinds of deformation behaviors are found for those GeNWs, depending on the strength of external loading. The first behavior is viewed as elastic deformation. The NWs retain their original atomic structures within a critical compressive force. The second behavior can be considered as plastic deformation. Under the external loading beyond the elastic limit, the NWs no longer retain their original structure and undergo dramatic structural deformation. For a long nanowire, the critical buckling load is [34]:

$$P_{cr} = \frac{\pi^2 EI}{(\mu L)^2} \quad (1)$$

where E, I, μ, and L are the effective elastic modulus, the cross sectional moment of inertia, coefficient of length, and the length of the NWs, respectively. Eq. (1) shows that the critical load is inversely proportional to the square of the length. The critical load versus the nanowire length obtained using MD simulation is shown in Fig. 7(c). Based on the simulations, the smaller critical load is required for buckling as the length of the GeNWs increases. The trend is in agreement with the Euler theory.

4 CONCLUSIONS

In summary, the buckling behaviors of [100]-, [110]-, [111]-, and [112]-oriented GeNWs under axial compression are studied based on MD simulations with Stillinger-Weber potential. It is found that the critical load decreases as temperature increases, and the buckling load is approximately linearly dependent on the strain rate, which indicates that the temperature and strain rate exert significant effects on the mechanical response of GeNWs under compression. Buckling load decreases with the increase of wire length, which is in agreement with the Euler theory.

REFERENCES

[1] S.Y. Bae, H.W. Seo, J. Park, et al. Triangular gallium nitride nanorodes [J]. Appl. Phys. Lett. 82:4564, 2003.

[2] S. Mathur, H. Shen, V. Sivakov, U. Werner. Germanium Nanowires and Core-Shell Nanostructures by Chemical Vapor Deposition of [Ge(C5H5)2] [J]. Chem. Mater. 16:2449, 2004.

[3] J. Diao, K.Gall, M.L. Dunn. Surface stress driven reorientation of gold nanowires [J]. Phys. Rev. B 70:075413, 2004.

[4] JING Yuhang, MENG Qingyuan. Compression of BN Nanotubes: A Molecular Dynamics Study [J]. Chinese Journal of Computational Physics, 26:281, 2009.

[5] F. Xu, X. Liu, S.D. Tse, F. Cosandey, B.H. Kear. Flame synthesis of zinc oxide nanowires [J]. Chem. Phys. Lett. 449:175, 2007.

[6] SHEN Haijun, SHI Youjin. Thermal-stability and Tensile Properties of Single-walled Si-H Nanotubes [J]. Chinese Journal of Computational Physics, 25:92, 2008.

[7] P.V. Radovanovic, C.J. Barrelet, S. Gradecak, F. Qian, et al. General Synthesis of Manganese-Doped II-VI and III-V Semiconductor Nanowires [J]. Nano Lett. 5:1407, 2005.
[8] J.D. Holmes, K.P. Johnston, R.C. Doty, et al. Control of Thickness and Orientation of Solution-Grown Silicon Nanowires [J]. Science, 287:1471, 2000.
[9] D.D.D. Ma, C.S. Lee, F.C.K. Au, et al. Small-Diameter Silicon Nanowire Surfaces [J]. Science, 299:1874, 2003.
[10] R.S. Friedman, M.C. McAlpine, D.S. Ricketts, et al. High-speed integrated nanowire circuits [J]. Nature 434:1085, 2005.
[11] X. Zhao, C.M. Wei, L. Yang, et al. Quantum Confinement and Electronic Properties of Silicon Nanowires [J]. Phys. Rev. Lett. 92:236805, 2004.
[12] R. Kagimura, R.W. Nunes, H. Chacham. Structures of Si and Ge Nanowires in the Subnanometer Range [J]. Phys. Rev. Lett. 95:115502, 2005.
[13] R. Rurali, N. Lorente. On the properties of surface reconstructed silicon nanowires [J]. Nanotechnology, 16:S250, 2005.
[14] P.W. Leu, B. Shan, K. Cho, Surface chemical control of the electronic structure of silicon nanowires: Density functional calculations [J]. Phys. Rev. B 74:195320, 2006.
[15] J. Li and A.J. Freeman. First-principles determination of the electronic structures and optical properties of one-nanometer (001) and (111) Si nanowires [J]. Phys. Rev. B, 74:075333, 2006.
[16] Pavel B. Sorokin, Pavel V. Avramov, Alexander G. Kvashnin, et al. Density functional study of <110>-oriented thin silicon nanowires [J]. Phys. Rev. B, 77: 235417, 2008.
[17] P. Nguyen, H.T. Ng, M. Meyyappan. Growth of Individual Vertical Germanium Nanowires [J]. Adv. Mater. 17:549, 2005.
[18] T. Hanrath and B.A. Korgel. Crystallography and Surface Faceting of Germanium Nanowires [J]. Small, 1:717, 2005.
[19] Jessica L. Lensch-Falk, Eric R. Hemesath, Francisco J. Lopez, et al. Vapor-Solid-Solid Synthesis of Ge Nanowires from Vapor-Phase-Deposited Manganese Germanide Seeds [J]. J. Am. Chem. Soc. 129:10670, 2007.
[20] Eli Sutter, Birol Ozturk, Peter Sutter. Selective growth of Ge nanowires by low-temperature thermal evaporation [J]. Nanotechnology, 19:435607, 2008.
[21] R. Kagimura, R.W. Nunes, H. Chacham. Structures of Si and Ge Nanowires in the Subnanometer Range [J]. Phys. Rev. Lett. 95:115502, 2005.
[22] R. Haight, G. Sirinakis, M. Reuter. Photoelectron spectroscopy of individual nanowires of Si and Ge [J]. Appl. Phys, Lett. 91:233116, 2007.
[23] H. Adhikari, A.F. Marshall, C.E.D. Chidsey, P.C. Mclntyre. Germanium Nanowire Epitaxy: Shape and Orientation Control [J]. Nano Lett. 6:318, 2006.
[24] C.K. Chan, X.F. Zhang, Y. Cui. High Capacity Li Ion Battery Anodes Using Ge Nanowires [J]. Nano Lett. 8:307, 2008.
[25] D. Medaboina, V. Gade, S.K.R. Patil, S.V. Khare. Effect of structure, surface passivation, and doping on the electronic properties of Ge nanowires: A first-principles study [J]. Phys. Rev. B, 76:205327, 2007.
[26] F. Stillinger, T. Weber. Computer simulation of local order in condensed phases of silicon [J]. Phys. Rev. B, 31:5262, 1985.
[27] K. Ding and H.C. Andersen, Molecular-dynamics simulation of amorphous germanium [J]. Phys. Rev. B, 34:6987, 1986.
[28] M. Menon, D. Srivastava, I. Ponomareva, et al. Nanomechanics of silicon nanowires [J]. Phys. Rev. B, 70: 125313, 2004.
[29] I. Ponomareva, M. Menon, D. Srivastava, et al. Structure, Stability, and Quantum Conductivity of Small Diameter Silicon Nanowires [J]. Phys. Rev. Lett. 95: 265502, 2005.
[30] X.W. Liu, J. Hu, B.C. Pan. The composition-dependent mechanical properties of Ge/Si core-shell nanowires [J]. Physica E, 40:3042, 2008.
[31] H.Andersen. Molecular dynamics simulations at constant pressure and/or temperature [J] J.Chem.Phys. 72:2384, 1980.
[32] L.T. Ngo, D. Almecija, J.E. Sader, et al. Ultimate-Strength Germanium Nanowires [J]. Nano Lett. 6:2964, 2006.
[33] Damon A. Smith, Vincent C. Holmberg, Doh C. Lee, Brian A. Korgel. Young's Modulus and Size-Dependent Mechanical Quality Factor of Nanoelectromechanical Germanium Nanowire Resonators [J]. J. Phys. Chem. C, 112:10725, 2008.
[34] S.P. Timoshenko, J.M. Gere, Theory of Elastic Stability [M], 2nd edition, McGraw-Hill, New York, 541, 1961.